*Cerebral Cortex*, June 2019;29: 2575–2587

**doi: 10.1093/cercor/bhy126**
Advance Access Publication Date: 18 May 2018
Original Article

ORIGINAL ARTICLE

# A Longitudinal Study of Local Gyrification Index in Young Boys With Autism Spectrum Disorder

Lauren E. Libero[1], Marie Schaer[2], Deana D. Li[1], David G. Amaral[1] and Christine Wu Nordahl[1]

[1]UC Davis MIND Institute and the UC Davis Department of Psychiatry and Behavioral Sciences, School of Medicine, 2230 Stockton Blvd., Sacramento, CA 95817, USA and [2]Office Medico-Pedagogique, Universite de Geneve, Rue David Dafour 1, 1205 Geneva 8, Switzerland

Address correspondence to Lauren E. Libero, University of California, Davis MIND Institute, 2825 50th Street, Sacramento, CA 95817, USA. Email: lelibero@ucdavis.edu

## Abstract

Local gyrification index (LGI), a metric quantifying cortical folding, was evaluated in 105 boys with autism spectrum disorder (ASD) and 49 typically developing (TD) boys at 3 and 5 years-of-age. At 3 years-of-age, boys with ASD had reduced gyrification in the fusiform gyrus compared with TD boys. A longitudinal evaluation from 3 to 5 years revealed that while TD boys had stable/decreasing LGI, boys with ASD had increasing LGI in right inferior temporal gyrus, right inferior frontal gyrus, right inferior parietal lobule, and stable LGI in left lingual gyrus. LGI was also examined in a previously defined neurophenotype of boys with ASD and disproportionate megalencephaly. At 3 years-of-age, this subgroup exhibited increased LGI in right dorsomedial prefrontal cortex, cingulate cortex, and paracentral cortex, and left cingulate cortex and superior frontal gyrus relative to TD boys and increased LGI in right paracentral lobule and parahippocampal gyrus, and left precentral gyrus compared with boys with ASD and normal brain size. In summary, this study identified alterations in the pattern and development of LGI during early childhood in ASD. Distinct patterns of alterations in subgroups of boys with ASD suggests that multiple neurophenotypes exist and boys with ASD and disproportionate megalencephaly should be evaluated separately.

**Key words:** autism, autism spectrum disorder, autistic, brain development, cortical folding, gyrification, longitudinal, MRI

Gyrification is the process of forming sulci and gyri in the mammalian cerebral cortex, with peaks becoming gyri and troughs becoming sulci. One strategy developed to quantify the degree of gyrification is the calculation of the local gyrification index (LGI), a metric that quantifies the ratio of inner sulcal folds compared with the outer smooth surface of the cortex (Schaer et al. 2008, 2012). A large LGI indicates extensive or deep folding, while small LGI indicates limited folding. This measure can be used to quantify differences in the pattern of cortical folding in neurodevelopmental disorders such as autism spectrum disorder (ASD), which manifests clinically during early childhood and is characterized by impairments in social communication and repetitive behaviors.

Gyrification mainly occurs during prenatal and early postnatal life, thus investigating LGI during early childhood in ASD may be valuable as a marker for alterations in the development of the cerebral cortex. Early prenatal neuronal proliferation provides the framework for the cortex and sets the stage for gyrification. In the first 6 weeks of fetal life, neuronal progenitor cells are rapidly generated in the subventricular zone (Rajkowska and Goldman-Rakic 1995), which then divide and migrate during weeks 6–12 to form the cortical plate (Sidman and Rakic 1973). These 2 phases of cell division mark the beginning of gray matter formation and ultimately determine both cortical thickness and surface area (White et al. 2010), and in turn affect gyrification. At 25 weeks

gestation, the cortical plate appears mostly smooth with no major sulci (Clouchoux et al. 2012). As development proceeds, cortical folding becomes more complex, with secondary sulci forming around 30 weeks and the degree of cortical folding increasing with gestational age (Clouchoux et al. 2012). In postnatal life, the brain continues to grow in size, and myelin production and synaptic pruning proceed throughout childhood and into adolescence. Previous studies of typical developmental have shown that there is a progressive increase in gyrification during the first 2 years of life, followed by a reduction in cortical folding complexity across the lifespan (White et al. 2010; Alemán-Gómez et al. 2013; Hogstrom et al. 2013; Mutlu et al. 2013; Klein et al. 2014; Li et al. 2014; Cao et al. 2017; Forde et al. 2017).

While alterations in cortical folding patterns have previously been reported in older individuals with ASD (Levitt et al. 2003; Hardan et al. 2004; Nordahl et al. 2007; Kates et al. 2009; Jou et al. 2010; Shokouhi et al. 2012; Schaer et al. 2013, 2015; Wallace et al. 2013; Libero et al. 2014; Bos et al. 2015; Dierker et al. 2015; Brun et al. 2016; Ecker et al. 2016; Yang et al. 2016), LGI has yet to be investigated in young children with ASD, close in time to the age of diagnosis. This is a critical period to investigate neural alterations related to ASD because it precedes the intensive behavioral and pharmacological interventions undergone by many individuals with ASD that likely alter brain structure and function. At older ages, it is difficult to determine whether neural alterations observed in individuals with ASD are related specifically to the neural alterations associated with the etiologies of the disorder or to compensatory changes that have occurred following interventions. The current study investigates differences in LGI and LGI development in a large cohort of boys enrolled in the ongoing Autism Phenome Project (APP), a longitudinal, multidisciplinary study aimed at identifying and characterizing different biological phenotypes of ASD, who received a first MRI between 2 and 3½ years of age and subsequent MRIs 1 and 2 years later. This cohort represents the entire range of symptom severity and cognitive abilities in ASD, and is compared with an age-matched typically developing (TD) group. We examined LGI at 3 years of age, as well as the change in LGI from 3 to 5 years of age.

One of the main goals of the APP is to identify clinically meaningful neurophenotypes of ASD. Previous work in this cohort has described a subgroup of boys with ASD (about 15% of the cohort) who have brain enlargement that is disproportionate to height. We call this group ASD with disproportionate megalencephaly (ASD-DM) (Ohta et al. 2015; Libero et al. 2016; Amaral et al. 2017). Clinically, boys with this neurophenotype have lower language ability at 3 years of age and have made fewer intellectual quotient (IQ) gains by age 5 compared with their counterparts with ASD and brain size in the normal range. Specifically, by age 5, the ASD-DM subgroup had a lower mean IQ score than other children with ASD (68 vs. 84) and a higher proportion of children with ASD-DM had IQ scores in the range of intellectual disability (IQ < 70) than other children with ASD (64% vs. 31%) (Amaral et al. 2017). Investigations into the neural basis of this phenotype reveal that brain enlargement that is disproportionate to height persists across early childhood (Libero et al. 2016) and that brain enlargement is regionally specific (Ohta et al. 2015). Based on this evidence, a secondary aim of the current study was to evaluate whether boys with ASD-DM also exhibit distinct patterns of gyrification. We hypothesize that ASD-DM will demonstrate a different pattern of LGI which would provide evidence that this subgroup represents a distinct neurophenotype of ASD.

## Materials and Methods

### Participants and Subgroups of ASD

Participants were enrolled in the ongoing University of California, Davis Medical Investigation of Neurodevelopmental Disorders (MIND) Institute APP. Participants with ASD were recruited through the MIND Institute clinic, California Regional Centers, and local clinics and community events. TD participants were recruited through community events and health fairs. At entry to the study (Time 1), participants are 2–3.5 years-of-age, and MRI and behavioral data are collected. Longitudinal MRIs are collected 1 year later (Time 2). A third MRI and additional behavioral data are collected 1 year later at Time 3 when children are around 5 years of age. In the current study, we are including data from Times 1 and 3, when MRI and concurrent behavioral data were collected.

Participants included 105 male children with ASD and 49 TD boys at Time 1. A subset of 52 ASD and 28 TD boys returned at Time 3. At Time 1, boys with disproportionate megalencephaly were classified based on criteria previously established (Ohta et al. 2015; Libero et al. 2016; Amaral et al. 2017): having a ratio of total cerebral volume (TCV) to height that is 1.5 standard deviations above the mean of sex-matched TD controls. The ratio of brain size to height is used because previous studies report body size enlargement in ASD (Davidovitch et al. 1996; Lainhart et al. 1997; Miles et al. 2000; Dissanayake et al. 2006; Chawarska et al. 2011), which could bias groupings based on brain size alone as taller individuals tend to have larger brains (Weinberg et al. 1974; Gould 1981; Jones and Lewis 1991; Lainhart et al. 2006). Based on this classification, 17 of the ASD participants were classified as ASD-DM and the remaining 88 ASD participants were classified as having brain size within the normal range (ASD-N). Two TD participants were classified as DM and were included in analyses as TD. At Time 3, the sample included 41 boys with ASD-N and 11 boys with ASD-DM. None of the participants with ASD changed classifications from Time 1 to Time 3. Targeted sequencing for ASD risk genes (see (Coe et al. 2014) for list of specific candidate genes) was carried out in the ASD-DM participants. One ASD-DM participant was identified to have a loss of function CHD8 mutation (and is included in a previous paper (Bernier et al. 2014)). None of the other ASD-DM participants had any known genetic risk for macrocephaly/megalencephaly. Data from these participants have been reported previously (Nordahl et al. 2011, 2012, 2013, 2015; Ohta et al. 2015; Libero et al. 2016).

When this study began, the sample size of females with ASD was insufficient to evaluate sex differences in LGI. Since there is growing evidence for sex differences in brain organization in girls with ASD (Lai et al. 2013; Nordahl et al. 2015; Schaer et al. 2015; Ecker et al. 2017), MRI scans from the girls participating in the APP were not included in the current study. All aspects of the study protocol were approved by the University of California, Davis Institutional Review Board, and informed consent was obtained from the parent or guardian of each participant.

Diagnostic measures included the Autism Diagnostic Observation Scale-Generic (ADOS-G) (DiLavore et al. 1995; Lord et al. 2000) and the Autism Diagnostic Interview-Revised (ADI-R) (Lord et al. 1994), conducted by trained, licensed clinical psychologists who specialize in autism and were research reliable for these tools. Inclusion criteria for ASD were based on the diagnostic definition of ASD in young children established by the Collaborative Programs of Excellence in Autism network using

DSM-IV (American Psychiatric Association 1994) criteria. Participants met ADOS-G cutoff scores for either autism or ASD. In addition, they exceeded the ADI-R cutoff score for autism on either the Social or Communication subscale and were within 2 points of this criterion on the other subscale. ADOS severity scores were calculated to allow comparison of autism severity across participants tested with different ADOS-G modules (Gotham et al. 2009). At Time 1, developmental quotient (DQ) for all participants was measured using the Mullen Scales of Early Learning (MSEL) (Mullen 1995). At Time 3, DQ was estimated using the General Conceptual Ability composite from the Differential Ability Scales-II (DAS-II) (Elliott 2007). Children who were unable to achieve a basal score on the DAS-II were administered the MSEL, and a ratio DQ was calculated by averaging age equivalents from the Fine Motor, Visual Reception, Expressive Language, and Receptive Language subscales, dividing by the child's chronological age and multiplying by 100. At both baseline and longitudinal follow-up, other measures collected include the Social Responsiveness Scale (SRS) (Constantino and Gruber 2002), Repetitive Behavior Scale-Revised (RBS-R) (Lam and Aman 2007), and the Vineland Adaptive Behavior Scales-II (VABS-II) (Sparrow et al. 1989). At Time 1, TD boys were screened for autism traits using the Social Communication Questionnaire (SCQ) (scores below 11) (Rutter et al. 2003). Only TD boys who had developmental scores within 2 standard deviations on all scales of the MSEL were included in this study. Three of the TD boys had elevated SCQ scores at Time 1 (2 boys scored 11, and one boy scored 12). ASD was ruled out in all 3 of these cases through additional administration of the ADOS-G. All participants were native English speakers, ambulatory, had no vision or hearing problems, no other neurological conditions and were able to complete an MRI study during sleep.

## Neuroimaging

MRI was carried out at the UC Davis Imaging Research Center using a 3T Siemens TIM Trio MRI scanner (Siemens Medical Solutions, Erlangen, Germany) with an 8-channel head coil. MRI scans were conducted during natural nocturnal sleep (Nordahl et al. 2008). T1-weighted 3D sagittal MPRAGE scans (TR = 2170 ms, TE = 4.86 ms, matrix size = 256 × 256, slice thickness = 1.0 mm, isotropic voxel size = 1 mm) were acquired for each child. T2-weighted images were also collected and reviewed by a pediatric neuroradiologist to rule out clinically significant findings.

A calibration phantom (ADNI MAGPHAN, Phantom Laboratory, Inc., Salem, New York) was scanned at the end of each MRI session using an MPRAGE pulse sequence matched to the study sequence and using the same landmark and shim as the corresponding participant to ensure accurate measurement of spatial characteristics of the MRI volume. A 3D image distortion map was derived to correct for hardware-induced geometric distortion (Image Owl, Inc., Salem, NY, routine previously described in (Nordahl et al. 2012)).

## Image Processing

After distortion correction, images were preprocessed by removing nonbrain tissue and correcting image intensity nonuniformity (inhomogeneity). An automated template-based method was used to measure TCV (total gray and white matter tissue, excluding cerebellum and brain stem) to identify which cases have disproportionate megalencephaly according to procedures described previously (Nordahl et al. 2011, 2012) and consistent with our previous groupings of ASD-DM (Ohta et al. 2015; Libero et al. 2016; Amaral et al. 2017).

Participants' distortion corrected structural MRI images were visually inspected slice-wise for motion, grainy images, ringing or Gibbs artifact that blurred the boundaries (contrast) between gray matter and white matter tissues. If any of these artifacts were present on at least one 2D image slice, the entire 3D structural MRI did not pass inspection. At Time 1, no images were excluded and at Time 3, 2 of the 11 ASD-DM cases were excluded for motion (these cases are not included in the final number of subjects [reported in Table 3]). Approved quality checked MRIs were then segmented using FreeSurfer 5.1 (http://surfer.nmr.mgh.harvard.edu) (Fischl and Dale 2000; Fischl 2012). Previous publications detail the technical aspects of this procedure (Dale and Sereno 1993; Dale et al. 1999; Fischl, Sereno and Dale 1999; Fischl, Sereno, Tootell, et al. 1999; Fischl and Dale 2000, 2001; Fischl et al. 2004; Ségonne et al. 2004; Han et al. 2006; Jovicich et al. 2006). In short, FreeSurfer computes, for each subject, a cortical surface meshes that represent the inner cortical surface (gray-white boundary, "white surface") and the outer cortical surface (gray-CSF boundary, "pial surface"). The segmented images were visually inspected for accuracy of surface reconstruction. If the automated segmentation steps resulted in errors (improper skull stripping, incorrect placement of gray matter-white matter or gray matter-CSF boundaries, or inclusion of nonbrain matter as cortex), manual corrections were performed. These manual edits were performed on every case, resulting in no remaining segmentation errors, and all data were included for statistical analyses. LGI was computed as a ratio between the pial surface of cortex and the constructed smooth outer surface covering the cerebrum (in a simplified form: pial surface [sulcal folds]/outer surface [smooth surface "hull"]) using a sampling sphere with the default 25 mm radius (Schaer et al. 2008) (Fig. 1). All scans were registered to a common space using spherical registration of the surfaces to the *fsaverage* template space that minimizes metric distortion and allows for a highly reliable point-to-point (at each vertex across the entire surface of the brain) comparison of cortical measures between groups (Fischl, Sereno and Dale 1999; Fischl, Sereno, Tootell, et al. 1999). As the LGI measure is already intrinsically smooth, the data were only minimally smoothed, using a Full Width at Half Maximum (FWHM) 2D Gaussian kernel of 1 mm to achieve an overall smoothness degree of 15 mm.

The standard FreeSurfer longitudinal pipeline was created for studies in adults and is based on within-subject template estimation (Reuter et al. 2012), which assumes there may be minimal changes in the cortical surface with age but no large changes in overall head or brain size. Given the substantial volumetric changes occurring from age 3 to 5 years, using this pipeline to assess our cohort introduces significant distortion and inconsistencies. For the longitudinal analyses, we instead registered each subject directly to the *fsaverage* subject and computed change in LGI (ΔLGI) as LGI at Time 3—LGI at Time 1 for each individual participant. A ΔLGI of 0 would represent no change in LGI over time.

## Statistical Analyses

Groups were compared on age, DQ, SRS total *t*-score, RBS-R total score, VABS-II adaptive behavior composite score, and TCV using ANCOVA (age as a covariate). Cross-sectional group comparisons were made using a general linear model design correcting for age and total brain volume as calculated by FreeSurfer (supratentorial volume) at each vertex. These comparisons included all ASD versus TD, ASD-N versus TD, ASD-N

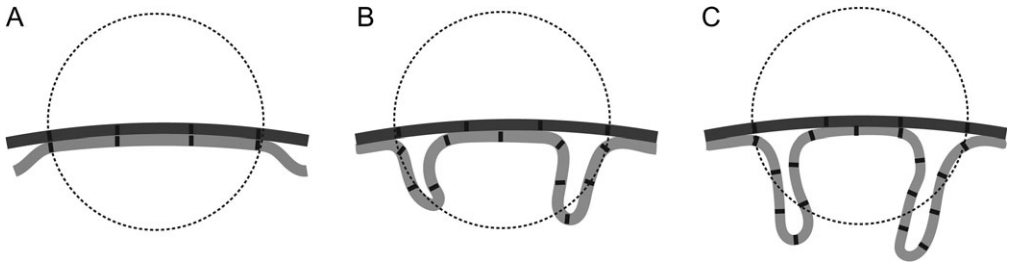


**Figure 1.** 2D schematic illustration of LGI calculation. Within a circular region where a sphere intersects the surface of the brain (dotted line), LGI is computed as a ratio between the actual curved pial surface (light gray line) and a constructed smooth outermost surface (dark gray line). LGI is calculated as pial surface divided by outer surface. The resulting LGI value represents the degree to which the cortical surface is curved and folded rather than smooth. The illustration represents 3 levels of LGI: (A) The pial surface is mostly smooth with little folding (LGI: 3/3 = 1.0). (B) The pial surface has distinct cortical folds, resulting in an average level of LGI (LGI: 9/3 = 3.0). (C) The pial surface is highly convoluted, with a high degree of cortical folding and high LGI (LGI: 15/3 = 5.0).

versus ASD-DM, and ASD-DM versus TD. To examine developmental effects, we compared ΔLGI across the whole brain for the subgroup of boys who have MRI data collected at both baseline and longitudinal visits. We examined ΔLGI in the ASD subgroups separately because, based on the Time 1 results, boys with ASD-DM were found to have a markedly different pattern of LGI. Although their alterations do not seem to influence the whole group, we nevertheless keep them separate because of their differences at Time 1. For all vertex-wise analyses, we used a cluster-forming statistical threshold of $P < 0.05$ corrected for multiple comparisons using Monte Carlo simulations (Hagler et al. 2006).

Because surface area is highly correlated with cortical folding and brain size (Pakkenberg and Gundersen 1997; Im et al. 2008; Hogstrom et al. 2013) and could provide additional evidence for cortical alterations related to brain size in ASD, we conducted post hoc analyses of surface area within the regions found to have significant alterations in LGI between groups. The boundaries of each region on the *fsaverage* space were saved as region label files. Each region label was then transformed from the *fsaverage* space to each subject's individual FreeSurfer anatomical space. Subject-specific surface area measurements were then calculated within the bounds of each region and compared between groups.

For each brain region with a significant difference in LGI between groups, subjects' individual LGI values were extracted at the vertex showing the highest significant group difference. These LGI values were correlated with the following clinical measures: ADOS-G severity score and subscale scores, SRS total t-score, DQ, nonverbal DQ (NVDQ), verbal DQ (VDQ), RBS-R total score, VABS-II composite score, and VABS-II subscale scores. False Discovery Rate (FDR) was used for multiple comparison correction.

## Results

### Participant Characteristics

At Time 1, there were no significant differences between groups for age, but the groups did significantly differ on DQ, SRS total t-score, RBS total score, and VABS-II adaptive behavior composite scores. The TD group had higher DQ, fewer repetitive behaviors, and better social and adaptive functioning at Time 1 (Table 1). The boys with ASD (ASD-N and ASD-DM combined) had significantly greater brain volume than the TD boys. When comparing the boys with ASD-DM to the ASD-N group, the ASD-DM group had significantly greater brain volume, but no significant differences on any of the other measures (Table 2).

Similar behavioral differences as described above (at Time 1) were found at Time 3—the ASD-N and ASD-DM groups had significantly lower DQ, greater SRS total t-score, greater RBS total score, and lower VABS-II adaptive behavior composite scores, compared with the TD group, such that the ASD-N and ASD-DM groups had lower cognitive abilities, greater repetitive behaviors, and poorer social and adaptive functioning at Time 3. The ASD-DM group had significantly greater brain volume compared with both the ASD-N and TD groups (Table 3). No significant differences in the behavioral measures emerged between the ASD-N and ASD-DM groups, however the final sample of 9 boys with ASD-DM greatly reduced power to detect substantial differences. In a previous behavioral study that included a larger sample of boys, we did detect differences in cognitive development between ASD-DM and ASD-N (Amaral et al. 2017).

### LGI at 3 Years-of-Age (Time 1)

A direct comparison of all boys with ASD to TD boys at Time 1 revealed reduced LGI in boys with ASD in regions involving portions of the left and right caudal fusiform gyrus and extending into the inferior temporal cortex (Fig. 2 and Table 4).

Next, we evaluated each subgroup of ASD boys (ASD-N and ASD-DM) separately relative to TD controls. Similar to the results of all boys with ASD relative to TD controls, the boys in the ASD-N group, when compared with TD boys, had significantly reduced LGI in the left and right fusiform gyrus extending into inferior temporal cortex, which is similar to the finding when all boys with ASD are compared with the TD group. The ASD-N boys did not show any areas of increased LGI.

In contrast, when the ASD-DM group was compared separately with TD boys, a different pattern of LGI alterations emerged. The boys with ASD-DM had significantly increased LGI in 2 large right medial hemisphere regions encompassing a large portion of the dmPFC and expanding into the anterior cingulate cortex and paracentral gyrus. In the left hemisphere, regions of increased LGI involved the entire cingulate gyrus and extended into dmPFC and superior frontal gyrus (Fig. 3 and Table 4). The ASD-DM boys did not show LGI alterations within the fusiform gyrus area, suggesting that this group represents a distinct neurophenotype from the boys with ASD-N.

Indeed, when the ASD-N group was compared directly to the ASD-DM group, the ASD-DM group had significantly greater LGI in 3 regions: one comprising the right paracentral lobule, one encompassing the right inferior temporal gyrus, parahippocampal gyrus and the caudal part of the entorhinal cortex, and one covering part of the left precentral and postcentral gyri.

**Table 1** Participant characteristics at Time 1 for boys with ASD and TD boys

| | ASD | TD | F-value | P-value |
|---|---|---|---|---|
| N | 105 | 49 | – | – |
| Age (months) | 36.01 (5.28) | 35.78 (4.77) | 0.066 | 0.797 |
| Age range | 25.6–44.0 | 27.2–44.0 | – | – |
| DQ | 63.62 (21.3) | 105.20 (11.7) | 158.6 | <0.001 |
| ADOS-G severity score | 7.84 (1.77) | – | – | – |
| SRS total | 78.20 (10.1) | 46.93 (6.71) | 358.6 | <0.001 |
| RBS-R total | 26.87 (14.7) | 5.56 (6.5) | 76.0 | <0.001 |
| VABS-II composite total | 75.73 (13.8) | 111.1 (13.2) | 212.6 | <0.001 |
| Total cerebral volume ($cm^3$) | 1028.6 (86.0) | 985.5 (77.0) | 9.86 | 0.002 |

**Table 2.** Participant characteristics at Time 1 for the subgroups of boys with ASD: ASD-DM and ASD-N

| | ASD-N | ASD-DM | F-value | P-value |
|---|---|---|---|---|
| N | 88 | 17 | – | – |
| Age (months) | 36.01 (5.34) | 36.05 (5.10) | 0.001 | 0.974 |
| Age range | 25.6–44.0 | 26.0–44.0 | – | – |
| DQ | 64.26 (21.27) | 58.64 (22.72) | 0.963 | 0.329 |
| ADOS-G severity score | 7.88 (1.72) | 7.65 (2.06) | 0.230 | 0.633 |
| SRS total | 76.55 (13.58) | 81.06 (9.01) | 1.68 | 0.197 |
| RBS-R total | 27.16 (15.59) | 25.62 (10.39) | 0.103 | 0.749 |
| VABS-II composite total | 76.84 (11.32) | 70.35 (22.16) | 3.14 | 0.080 |
| Total cerebral volume ($cm^3$) | 1007.11 (72.60) | 1140.13 (60.50) | 62.21 | <0.001 |

**Table 3.** Participant characteristics for the subset of boys with ASD-N, ASD-DM, and TD boys who were followed longitudinally from Time 1 (3 years of age) to Time 3 (5 years of age)

| | Time 1 | | | Time 3 | | |
|---|---|---|---|---|---|---|
| | TD | ASD-N | ASD-DM | TD | ASD-N | ASD-DM |
| N | 28 | 41 | 9 | 28 | 41 | 9 |
| Age (months) | 35.34 (4.50) | 35.38 (5.50) | 35.73 (5.65) | 61.71 (5.16) | 62.70 (5.20) | 61.13 (6.41) |
| Age range | 27.2–42.9 | 26.9–44.0 | 26.0–44.0 | 53.1–69.6 | 54.6–71.9 | 52.0–69.7 |
| Scan interval (months) | – | – | – | 26.36 (1.55) | 27.10 (2.20) | 25.39 (5.31) |
| Scan interval range | – | – | – | 22.7–32.5 | 24.0–30.5 | 16.27–34.2 |
| DQ | 104.59 (11.46) | 64.73 (22.53)[a] | 65.68 (24.70)[b] | 111.41 (9.02) | 82.13 (32.7)[a] | 74.50 (35.14)[b] |
| ADOS-G Severity Score | – | 7.83 (1.82) | 7.11 (2.36) | – | 7.16 (2.15) | 6.67 (3.00) |
| SRS total | 47.15 (6.35) | 77.83 (10.39)[a] | 81.11 (10.57)[b] | 45.92 (5.86) | 74.45 (11.27)[a] | 80.13 (16.20)[b] |
| RBS-R total | 5.04 (6.67) | 27.90 (16.81)[a] | 29.17 (13.36)[b] | 3.54 (6.00) | 26.19 (12.74)[a] | 34.00 (21.12)[b] |
| VABS-II composite total | 110.37 (11.88) | 76.20 (10.68)[a] | 71.56 (29.35)[b] | 108.85 (11.20) | 76.91 (17.30)[a] | 73.63 (18.66)[b] |
| Total cerebral volume ($cm^3$) | 991.25 (76.64) | 1017.08 (62.37) | 1152.14 (54.40)[b,d] | 1070.28 (81.39) | 1085.18 (59.79) | 1181.62 (42.83)[b,c] |

Note. Significant contrast between TD and ASD-N [a]$P < 0.001$; significant contrast between TD and ASD-DM [b]$P < 0.001$; significant contrast between ASD-N and ASD-DM [c]$P < 0.005$, [d]$P < 0.001$.

## LGI Changes During Development

To examine developmental trajectories, the change in LGI (ΔLGI) between Time 1 and Time 3 was examined. Since the cross-sectional analyses at Time 1 suggested that ASD-N and ASD-DM groups exhibit different patterns of gyrification relative to TD controls, the groups were evaluated separately for longitudinal change. Comparison of the ASD-N and TD groups revealed significantly different patterns of LGI development with age in 4 regions. These regions include the right inferior frontal gyrus, the right inferior temporal gyrus, the right inferior parietal lobule, and the left lingual gyrus (Fig. 4 and Table 4) Individual and group-averaged trajectories for each of these regions are depicted in Supplementary Figure S1. In TD boys, within these 4 regions, ΔLGI was either negative or close to zero (signifying decreasing or stable LGI from 3 to 5 years-of-age). In contrast, LGI increased in right inferior frontal gyrus, right inferior temporal gyrus, and right inferior parietal lobule, and was stable in left lingual gyrus in boys with ASD-N.

No significant differences were found in the longitudinal changes in LGI between boys with ASD-DM and boys with ASD-N or TD boys when accounting for multiple comparisons. However, these analyses were underpowered with only 9 boys with ASD-DM included at Time 3.

In order to facilitate comparison of the current results with other literature on 5-year-olds, we also conducted a cross-sectional analysis of the subset of 84 boys with available Time

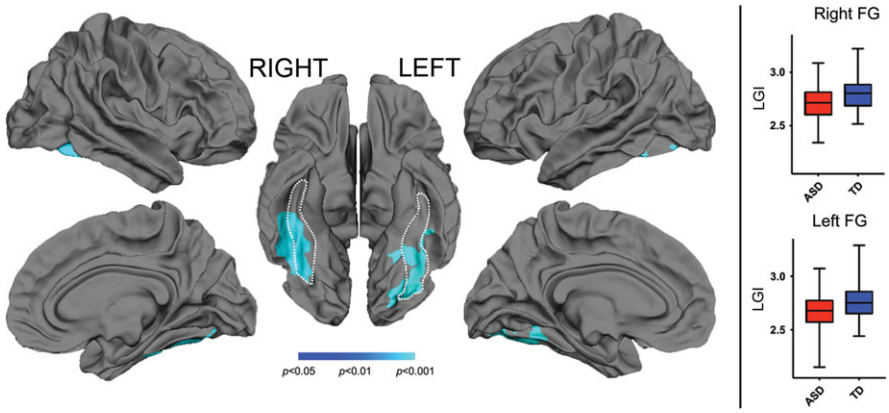


**Figure 2.** Regions (blue profiles) of reduced LGI in boys with ASD at Time 1 (approximately 3 years-of-age). Boys with ASD had significantly reduced LGI in portions of the left and right caudal fusiform gyrus (FG), extending into inferior temporal cortex, compared with TD boys. The boundaries of the whole FG are indicated with white dotted line. On the right side, boxplots show LGI data for each group at the vertex of highest significant difference between groups located in left and right FG.

**Table 4.** Brain regions with significant group differences in LGI for TD boys, all boys with ASD, and the 2 subgroups of boys with ASD (ASD-DM and ASD=N)

| Comparison | Anatomical region | Left/ right | Area ($mm^2$) | Talairach coordinates (x,y,z) | Cluster-wise P-value | Direction |
|---|---|---|---|---|---|---|
| ASD versus TD | Fusiform gyrus | Right | 1352.16 | 45, −33, −15.4 | 0.00120 | ASD < TD |
| | Fusiform gyrus | Left | 1412.97 | −25.6, −78.8, −2.8 | 0.0007 | ASD < TD |
| ASD-DM versus ASD-N | Paracentral gyrus | Right | 1766.45 | 15.3, −32.2, 66.9 | 0.0001 | ASD-DM > ASD-N |
| | Parahippocampal gyrus | Right | 2431.14 | 15.8, −39.4, −1.5 | 0.0001 | ASD-DM > ASD-N |
| | Precentral gyrus | Left | 2922.32 | −34.8, −13.2, 61.3 | 0.0001 | ASD-DM > ASD-N |
| ASD-DM versus TD | Dorsomedial prefrontal cortex | Right | 4934.29 | 17.6, 4.6, 58.4 | 0.0001 | ASD-DM > TD |
| | Cingulate cortex | Left | 4173.96 | −5.1, −7.4, 37.0 | 0.0001 | ASD-DM > TD |
| ASD-N versus TD | Fusiform gyrus | Right | 1603.10 | 45.9, −32.6, −15.8 | 0.0004 | ASD-N < TD |
| | Fusiform gyrus | Left | 1792.30 | −26.1, −78.7, −3.1 | 0.0001 | ASD-N < TD |
| Longitudinal ASD-N versus TD | Inferior parietal lobule | Right | 3244.79 | 44.6, −56.6, 44.5 | 0.0001 | ASD increasing |
| | Inferior frontal cortex | Right | 2354.02 | 44.9, 10.9, 16.6 | 0.0001 | ASD increasing |
| | Inferior temporal cortex | Right | 1713.47 | 47.8, −57.6, 5.6 | 0.0001 | ASD increasing |
| | Lingual gyrus | Left | 1801.86 | −9.4, −61.9, 2.4 | 0.0001 | ASD stable |

3 MRI data. Results from this analysis of LGI at 5 years-of-age is included in Supplementary material and Supplementary Figure 2.

### Post Hoc Comparison of Surface Area

Post hoc comparisons of surface area in the regions of significant LGI difference between groups revealed significantly greater surface area in the combined ASD group (ASD-N and ASD-DM), compared with TD, in both left ($F = 13.001$, $P < 0.001$) and right ($F = 4.203$, $P = 0.042$) fusiform gyrus. For ASD-N versus TD, there was significantly increased surface area in the ASD-N group in the left fusiform gyrus ($F = 10.757$, $P = 0.001$), but not right fusiform gyrus ($F = 0.003$, $P = 0.955$). For the ASD-DM versus ASD-N comparison, the ASD-DM group had significantly greater surface area in all regions with significant group differences in LGI: left precentral gyrus ($F = 18.792$, $P < 0.001$), right inferior temporal cortex ($F = 15.843$, $P < 0.001$), and right paracentral cortex ($F = 22.712$, $P < 0.001$). For the ASD-DM versus TD comparison, the ASD-DM group had significantly greater surface area in the regions with significant group differences in LGI: right dorsomedial prefrontal cortex (dmPFC) ($F = 56.939$, $P < 0.001$), and left cingulate gyrus ($F = 43.866$, $P < 0.001$) (see Supplementary Table S1).

### Behavioral Correlations

No significant correlations between scores on any of the behavioral measures (ADOS-G severity score and subscale scores, SRS total t-score, DQ, VDQ, NVDQ, RBS-R total score, VABS-II composite score, and VABS-II subscale scores) and LGI emerged for either group for the regions identified in the ASD versus TD comparison or ASD-N versus TD comparison. Correlations for the remaining regions do not survive correction for multiple comparisons but are reported in the Supplementary material. At Time 1, these include a relationship between the right paracentral lobule LGI and repetitive behaviors in boys with ASD-N, and several correlations relating the left cingulate gyrus LGI with cognitive and adaptive abilities in boys with ASD-DM. From the longitudinal analyses, ASD boys who had greater increases in LGI in the inferior temporal cortex had better socialization, and for TD boys declining LGI in the right inferior frontal and temporal cortices was related to better cognitive and adaptive abilities.

## Discussion

The goal of this study was to investigate LGI development in young boys with ASD and a subgroup of boys with ASD with enlarged brains, that is, disproportionate megalencephaly. We

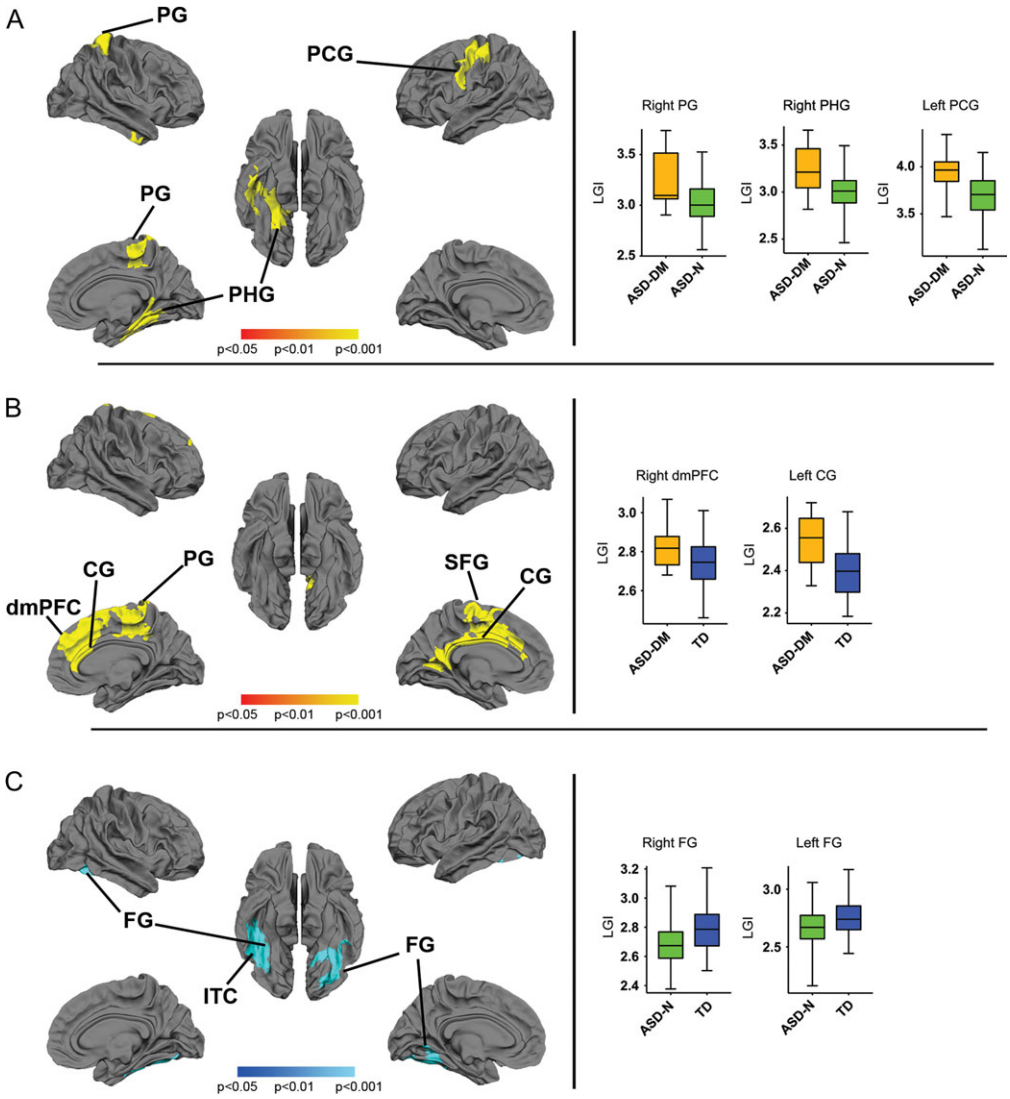


**Figure 3.** Regions with differing LGI between ASD-N, ASD-DM, and TD groups at Time 1. (*A*) Regions with increased LGI in boys with ASD-DM versus ASD-N. These regions include right paracentral gyrus (PG), right parahippocampal gyrus (PHG), and left precentral gyrus (PCG) and part of postcentral gyrus than boys with ASD-N. (*B*) Regions with increased LGI in boys with ASD-DM versus TD boys. These regions include right dmPFC, right cingulate gyrus (CG), right PG, left CG, and left superior frontal gyrus (SFG) compared with TD boys. (*C*) Regions of reduced LGI in boys with ASD-N versus TD boys. These regions include right and left fusiform gyrus (FG) and parts of inferior temporal cortices. On the right side, boxplots show LGI data for each group at the vertex of highest significant difference for each region with significant group differences.

have found that both the pattern and trajectory of cortical folding development is altered in preschool-aged boys with ASD. Consistent with the notion that there are various neurophenotypes of ASD (Amaral et al. 2017), we observed distinct patterns of cortical folding within 2 different subgroups of ASD that are defined based on brain size. In the majority of boys with ASD and brain size within the normal range (ASD-N), LGI is significantly reduced over the left and right caudal fusiform gyrus relative to TD boys. This pattern of reduced LGI in bilateral fusiform gyrus was not seen in the boys with ASD and disproportionate megalencephaly (ASD-DM). Rather, the subgroup of boys with ASD-DM have increased LGI in the right dmPFC and the left cingulate cortex relative to TD boys and increased LGI in the right paracentral lobule, right parahippocampal gyrus, and left precentral gyrus compared to boys with ASD-N. Longitudinal findings show that boys with ASD-N show a general increase in gyrification whereas TD boys have an unchanging or decreasing LGI in right inferior frontal cortex, right inferior parietal lobule, right inferior temporal cortex, and left lingual gyrus. In ASD-DM boys, we did not observe differences in the trajectory of LGI from TD or from ASD-N boys, but the analyses were underpowered with only 9 boys in the ASD-DM subgroup with longitudinal MRI data.

The findings of previous cross-sectional studies of LGI in ASD have provided varying results, including both reduced and increased LGI. Regions reported to have reductions in LGI in adolescent and adult participants with ASD include the inferior frontal gyrus, precentral gyrus, supramarginal gyrus, inferior parietal cortex, and cuneus/precuneus (Schaer et al. 2013; Libero et al. 2014). There is also one report of children and adults that found reduced LGI in ventromedial prefrontal cortex in males with ASD, but increased LGI in this area in females with ASD (Schaer et al. 2015). Regions reported to have increased LGI in children and adults include the central sulcus,

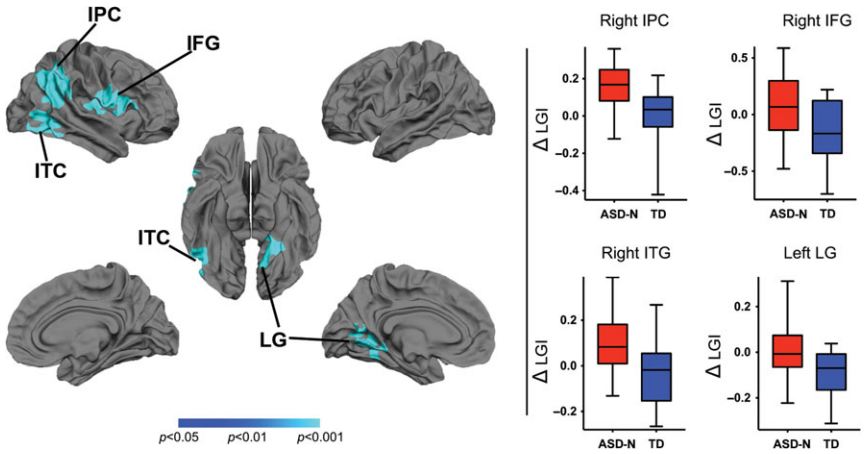


**Figure 4.** Differences in trajectory of LGI development in boys with ASD-N versus TD. Whereas change in LGI was negligible or negative for TD boys, the ASD-N group showed an increase in LGI in the same period. This pattern is most obvious in these 4 cortical regions: right inferior frontal gyrus (IFG), right inferior parietal cortex (IPC), right inferior temporal cortex (ITC), and left lingual gyrus (LG). The graphs depict boxplots of delta LGI data for each group at the vertex of highest significance difference within each region with significant group differences.

cingulate cortex, inferior parietal and temporal cortices, precuneus, lingual gyrus, and lateral occipital cortex (Wallace et al. 2013; Ecker et al. 2016; Yang et al. 2016). Finally, one study found no differences in LGI in adults with ASD (Koolschijn and Geurts 2016), and another found no direct group differences, but reported an age-dependent decrease in prefrontal and parietal cortices in adolescents with ASD (Bos et al. 2015).

Our current findings of alterations in gyrification in the ventral and medial temporal cortex do not overlap with regions identified in previous studies. However, the current study differs from previous studies of LGI in that it examines much younger boys with ASD during a relatively narrow age range of 3–5 years of age. Previous studies focused on older children, adolescents and adults with ASD. Our findings in very young children, close in time to the age of diagnosis, may represent the earliest manifestations of altered gyrification in ASD. Whether these alterations "normalize" over time, perhaps through compensatory processes related to intervention, and are thus not observed in older individuals with ASD remains unknown.

One of the main findings in the current study is that the majority of boys with ASD, those with normal brain size had bilateral reductions of LGI in portions of the fusiform gyrus. What are the implications of a reduction in LGI in the fusiform cortex? Structurally, this means that boys with ASD have less cortical folding in this region or a smoother gray matter surface. The fusiform gyrus is anatomically located medial to the occipitotemporal sulcus and lateral to the collateral sulcus. Alterations in the curvature of these sulci and the crown of the fusiform gyrus and/or the size and organization of the underlying white matter could impact the LGI pattern of this region. Functionally, the fusiform gyrus is critical to processing visual information related to complex objects including faces, and communicates with brain regions responsible for emotion and higher order social cognition (Kanwisher et al. 1997; McCarthy et al. 1997; Haxby et al. 2000, 2002; Kanwisher and Yovel 2006). Many previous functional MRI studies in ASD have found alterations in the activation of the fusiform gyrus as well as its functional connectivity (Critchley et al. 2000; Schultz et al. 2000; Pierce et al. 2001; Piggot et al. 2004; Wang et al. 2004; Kleinhans et al. 2008, 2016; Koshino et al. 2008; Lynn et al. 2016; Whyte et al. 2016). Behaviorally, the consequences of altered structure or connectivity of the fusiform gyrus in ASD may manifest in difficulties with facial recognition and memory (Weigelt et al. 2012). Although we did not observe clear associations between LGI and the standardized behavioral assessments administered through this study, it is possible that our measures were not sensitive enough to detect more specific associations between gyrification and functions known to be related to the fusiform gyrus.

The process of gyrification is not clearly understood although there are several theories of the formative processes. These theories can be grouped into 2 major camps. Differential tangential expansion theories of gyrification suggest that differential growth between regions or cortical layers leads to a buckling of the cortical sheet (His 1874; Retzius 1891; Clark WELG 1945; Richman et al. 1975; Toro and Burnod 2005; Todd 2013; Ronan et al. 2014) and formation of the characteristic patterns of sulci and gyri. The competing tension-based theory posits that neural connections forming in the second trimester produce local tension that pulls interconnected regions closer together (Van Essen 1997; Mota and Herculano-Houzel 2012). Based on this theory, the development of underlying white matter may contribute to the development of cortical folding. For boys with ASD-N, surface area was greater in the left fusiform gyrus but not different than TD boys in the right fusiform gyrus. In this case, more cortical surface is not generating more folds. Rather, boys with ASD-N had smoother fusiform cortex compared with controls. It is possible that reduced white matter tension underneath is flattening the gyrus, but this cannot be assessed in the current study. Although in vivo MRI lacks the resolution to investigate the cellular processes that underlie alterations in LGI, MRI studies can be used to direct the focus of microscopic cellular investigations of the cortical underpinnings of ASD (and determine whether differences may be due to greater cell proliferation or organization of cells or white matter). To date, only a few studies in ASD have examined the fusiform gyrus at a microanatomical level and none of these studies related cellular alterations to cortical folding. One postmortem study of the fusiform gyrus in ASD found reduced neuron densities in cortical layer III, reduced total neuron numbers in layers III, V, VI, and mean perikaryal volumes of neurons in layers V and VI (van Kooten et al. 2008). Cortical layer III is the principal source of association connections, and cortical layer V

is the main source of efferent connections to subcortical regions, suggesting there may be microstructural disconnection across the white matter network underlying the fusiform gyrus. However, another postmortem study in ASD reported no differences in neuronal density or cytoarchitecture of the fusiform gyrus in ASD (Oblak et al. 2011). In vivo, 2 diffusion MRI studies have reported alterations in the diffusion properties of the fusiform white matter pathways in ASD (Conturo et al. 2008; Sahyoun et al. 2010), supporting the possibility of disrupted structural connectivity of the fusiform gyrus, which could potentially reduce gyrification in the region. At this time, though, there is not enough evidence to conclude with certainty whether cellular and/or connectivity alterations at a microscopic level are driving alterations in gyrification in ASD.

Another novel finding from this study is that patterns of LGI alterations in boys with ASD are different in different subgroups based on brain size. The heterogeneity of ASD is widely recognized (Constantino and Charman 2016; Constantino 2018), and recent studies have focused on the importance of identifying subgroups or subtypes of ASD based on either behavioral or biological characteristics. In this study, we examined a subgroup of boys with disproportionately enlarged brains relative to their height. Increased head or brain size has long been observed in ASD (Piven et al. 1995; Lainhart et al. 1997; Courchesne et al. 2001; Redcay and Courchesne 2005), and our previous work has sought to determine whether individuals with ASD and disproportionately large brains represent a distinct and clinically meaningful neurophenotype of ASD (Nordahl et al. 2011; Ohta et al. 2015; Libero et al. 2016; Amaral et al. 2017). In the current study, we observed an altered pattern of cortical folding when compared not only to TD boys, but also to the boys with ASD with normal brain size. The patterns differed not only in regional specification, but also in the direction of the LGI. In contrast to decreases in gyrification observed in the majority of ASD boys with normal brain size, boys in the ASD-DM group exhibited increased gyrification. In addition, boys with ASD-DM had significantly greater surface area in all of the regions identified as having increased LGI. These findings are not particularly surprising, given that those with larger brains tend to have more gyrification and greater surface area (Armstrong et al. 1995; Pakkenberg and Gundersen 1997; Im et al. 2008). However, it should be noted that in the case of boys with ASD-DM, the degree of cortical folding was not increased across the entire cortex uniformly. Instead, LGI was increased specifically in the right dmPFC and left cingulate cortex relative to TD controls and more extensively in right paracentral lobule, right entorhinal cortex, parahippocampal gyrus, and inferior temporal gyrus, and left precentral gyrus compared to boys with ASD-N. The finding that boys with ASD-DM have a distinct pattern of cortical folding alterations provides further evidence that they represent a distinct subgroup of ASD.

In typical development, larger brains tend to have greater folding. And, increased cortical folding complexity is related to increased intelligence (Gregory et al. 2016). In the current study, we did not find a significant relationship between gyrification and cognitive abilities. For TD boys, declining LGI in right inferior frontal and temporal cortices was related to better cognitive and adaptive abilities. At an uncorrected level we found that in boys with ASD-DM, greater LGI in left cingulate gyrus was associated with greater DQ and adaptive living skills. For boys with ASD-N, greater LGI in right paracentral lobule LGI was associated with increased repetitive behaviors. Our uncorrected findings (see Supplementary material) also found ASD boys with greater increase in LGI across early childhood in inferior temporal cortex had better socialization abilities. Although regional alterations may translate to some behavioral differences, within the context of ASD, overall brain enlargement and increased cortical folding complexity does not seem to confer any major cognitive advantage.

A third interesting finding from this study is that boys with ASD-N showed increasing gyrification between 3 and 5 years of age compared to TD boys, who exhibited relatively stable or slightly decreasing LGI over this time period. In typical development, LGI is an age-dependent measure that changes over the lifespan—increasing within the first 2 years of life (Li et al. 2014), then decreasing from 4 years-of-age through adulthood (White et al. 2010; Alemán-Gómez et al. 2013; Hogstrom et al. 2013; Mutlu et al. 2013; Klein et al. 2014; Li et al. 2014; Cao et al. 2017; Forde et al. 2017). The reduction in LGI across the lifespan is driven by changes in curvature with age: across childhood and adulthood sulci become wider, shallower, and more flat, while gyri become steeper and more peaked (Magnotta et al. 1999; Rettmann et al. 2005; Kochunov et al. 2008, 2009; Pienaar et al. 2008; Alemán-Gómez et al. 2013). It is unclear exactly why cortical folding patterns change over time, but changes may reflect dynamic developmental processes. For example, ongoing synaptogenesis, synaptic pruning and progressive myelination alter cellular structure and the organization of gray and white matter (Huttenlocher 1979, 1982, 1999; Paus et al. 2001; Webb et al. 2001; Tau and Peterson 2010; Petanjek et al. 2011; Grydeland et al. 2013). In the current study, we found the expected pattern of decreasing or stable gyrification in TD boys, but in participants with ASD, the LGI increased over time. Further longitudinal examination of gyrification in ASD into middle childhood may explain whether the developmental curve is shifted (LGI development is delayed), or if the trajectory is altogether different in the context of ASD.

In summary, this study identified distinct patterns of altered gyrification in subgroups of boys with ASD based on brain size. Findings include reduced LGI in the caudal fusiform gyrus in young boys with ASD and normal brain size, and a pattern of increased LGI in boys with ASD and disproportionate megalencephaly. The current study also uncovered regional alterations in the trajectory of LGI across early childhood in boys with ASD. These findings emphasize the need for additional investigations following the same subjects across childhood and adolescence, to better understand cortical development in the context of ASD and its relationship to behavior. This study also highlights the importance of investigating subgroups of ASD. In this case, relative brain size has a significant impact on patterns of gyrification in ASD—indicating the need for studies separate analyses on individuals with ASD based on their neurophenotype.

## Supplementary Material

Supplementary material is available at *Cerebral Cortex* online.

## Funding

National Institute of Mental Health (1R01MH089626, 1R01MH103371, R01MH104438, U24MH081810) and the University of California Davis Medical Investigation of Neurodevelopmental Disorders (MIND) Institute. This project was also supported by the MIND Institute Intellectual and Developmental Disabilities Research Center (U54HD079125). Grants from the Swiss National Science Foundation (SNSF, 158831, 163859) to M.S. University of California President's Postdoctoral Fellowship to L.L.

## Notes

The authors would like to thank the families and children who are participating in the Autism Phenome Project study who have generously given their time to provide the data reported in this article. The authors thank Melissa Miller and Dr. Thomas Avino for their assistance with the figures. We also appreciate the conscientious critiques provided by 2 anonymous reviewers. *Conflict of Interest*: The authors do not declare any conflict of interest.

## References

Alemán-Gómez Y, Janssen J, Schnack H, Balaban E, Pina-Camacho L, Alfaro-Almagro F, Castro-Fornieles J, Otero S, Baeza I, Moreno D. 2013. The human cerebral cortex flattens during adolescence. J Neurosci. 33:15004–15010.

Amaral DG, Li DA, Libero L, Solomon M, Van de Water J, Mastergeorge A, Naigles L, Rogers S, Nordahl CW. 2017. In pursuit of neurophenotypes: the consequences of having autism and a big brain. Autism Res. 10:711–722.

American Psychiatric Association. 1994. DSM-IV: Diagnostic and statistical manual. Washington, DC: American Psychiatric Association.

Armstrong E, Schleicher A, Omran H, Curtis M, Zilles K. 1995. The ontogeny of human gyrification. Cereb Cortex. 5:56–63.

Bernier R, Golzio C, Xiong B, Stessman HA, Coe BP, Penn O, Witherspoon K, Gerdts J, Baker C, Vulto-van Silfhout AT. 2014. Disruptive CHD8 mutations define a subtype of autism early in development. Cell. 158:263–276.

Bos DJ, Merchán-Naranjo J, Martínez K, Pina-Camacho L, Balsa I, Boada L, Schnack H, Oranje B, Desco M, Arango C. 2015. Reduced gyrification is related to reduced interhemispheric connectivity in autism spectrum disorders. J Am Acad Child Adolesc Psychiatry. 54:668–676.

Brun L, Auzias G, Viellard M, Villeneuve N, Girard N, Poinso F, Da Fonseca D, Deruelle C. 2016. Localized Misfolding within Broca's area as a distinctive feature of autistic disorder. Biol Psychiatry Cogn Neurosci Neuroimaging. 1:160–168.

Cao B, Mwangi B, Passos IC, Wu M-J, Keser Z, Zunta-Soares GB, Xu D, Hasan KM, Soares JC. 2017. Lifespan gyrification trajectories of human brain in healthy individuals and patients with major psychiatric disorders. Sci Rep. 7:511.

Chawarska K, Campbell D, Chen L, Shic F, Klin A, Chang J. 2011. Early generalized overgrowth in boys with autism. Arch Gen Psychiatry. 68:1021–1031.

Clark WELG. 1945. Deformation patterns in the cerebral cortex: Printed at the Oxford University Press by John Johnson.

Clouchoux C, Kudelski D, Gholipour A, Warfield SK, Viseur S, Bouyssi-Kobar M, Mari J-L, Evans AC, Du Plessis AJ, Limperopoulos C. 2012. Quantitative in vivo MRI measurement of cortical development in the fetus. Brain Struct Funct. 217:127–139.

Coe BP, Witherspoon K, Rosenfeld JA, Van Bon BW, Vulto-van Silfhout AT, Bosco P, Friend KL, Baker C, Buono S, Vissers LE. 2014. Refining analyses of copy number variation identifies specific genes associated with developmental delay. Nat Genet. 46:1063.

Constantino JN. 2018. Deconstructing autism: from unitary syndrome to contributory developmental endophenotypes. Int Rev Psychiatry. 30:18–24.

Constantino JN, Charman T. 2016. Diagnosis of autism spectrum disorder: reconciling the syndrome, its diverse origins, and variation in expression. Lancet Neurol. 15:279–291.

Constantino JN, Gruber CP. 2002. The social responsiveness scale. Los Angeles: Western Psychological Services.

Conturo TE, Williams DL, Smith CD, Gultepe E, Akbudak E, Minshew NJ. 2008. Neuronal fiber pathway abnormalities in autism: an initial MRI diffusion tensor tracking study of hippocampo-fusiform and amygdalo-fusiform pathways. J Int Neuropsychol Soc. 14:933–946.

Courchesne E, Karns C, Davis H, Ziccardi R, Carper R, Tigue Z, Chisum H, Moses P, Pierce K, Lord C. 2001. Unusual brain growth patterns in early life in patients with autistic disorder an MRI study. Neurology. 57:245–254.

Critchley HD, Daly EM, Bullmore ET, Williams SC, Van Amelsvoort T, Robertson DM, Rowe A, Phillips M, McAlonan G, Howlin P. 2000. The functional neuroanatomy of social behaviour. Brain. 123:2203–2212.

Dale AM, Fischl B, Sereno MI. 1999. Cortical surface-based analysis: I. Segmentation and surface reconstruction. Neuroimage. 9:179–194.

Dale AM, Sereno MI. 1993. Improved localizadon of cortical activity by combining eeg and meg with mri cortical surface reconstruction: a linear approach. J Cogn Neurosci. 5: 162–176.

Davidovitch M, Patterson B, Gartside P. 1996. Head circumference measurements in children with autism. J Child Neurol. 11:389–393.

Dierker DL, Feczko E, Pruett JJR, Petersen SE, Schlaggar BL, Constantino JN, Harwell JW, Coalson TS, Van Essen DC. 2015. Analysis of cortical shape in children with simplex autism. Cereb Cortex. 25:1042–1051.

DiLavore PC, Lord C, Rutter M. 1995. The pre-linguistic autism diagnostic observation schedule. J Autism Dev Disord. 25: 355–379.

Dissanayake C, Bui QM, Huggins R, Loesch DZ. 2006. Growth in stature and head circumference in high-functioning autism and Asperger disorder during the first 3 years of life. Dev Psychopathol. 18:381–393.

Ecker C, Andrews D, Dell'Acqua F, Daly E, Murphy C, Catani M, de Schotten MT, Baron-Cohen S, Lai M, Lombardo M. 2016. Relationship between cortical gyrification, white matter connectivity, and autism spectrum disorder. Cereb Cortex. 26:3297–3309.

Ecker C, Andrews DS, Gudbrandsen CM, Marquand AF, Ginestet CE, Daly EM, Murphy CM, Lai M-C, Lombardo MV, Ruigrok AN. 2017. Association between the probability of autism spectrum disorder and normative sex-related phenotypic diversity in brain structure. Jama Psychiatry. 74: 329–338.

Elliott C. 2007. Differential ability scales. 2nd ed. New York: The psychological corporation.

Fischl B. 2012. FreeSurfer. Neuroimage. 62:774–781.

Fischl B, Dale AM. 2000. Measuring the thickness of the human cerebral cortex from magnetic resonance images. Proc Nat Acad Sci USA. 97:11050–11055.

Fischl B, Liu A, Dale AM. 2001. Automated manifold surgery: constructing geometrically accurate and topologically correct models of the human cerebral cortex. IEEE Trans Med Imaging. 20:70–80.

Fischl B, Salat DH, van der Kouwe AJ, Makris N, Ségonne F, Quinn BT, Dale AM. 2004. Sequence-independent segmentation of magnetic resonance images. Neuroimage. 23: S69–S84.

Fischl B, Sereno MI, Dale AM. 1999a. Cortical surface-based analysis: II: Inflation, flattening, and a surface-based coordinate system. Neuroimage. 9:195–207.

Fischl B, Sereno MI, Tootell RB, Dale AM. 1999b. High-resolution intersubject averaging and a coordinate system for the cortical surface. Hum Brain Mapp. 8:272–284.

Forde NJ, Ronan L, Zwiers MP, Schweren LJS, Alexander-Bloch AF, Franke B, Faraone SV, Oosterlaan J, Heslenfeld DJ, Hartman CA, et al. 2017. Healthy cortical development through adolescence and early adulthood. Brain Struct Funct. 222:3653–3663.

Gotham K, Pickles A, Lord C. 2009. Standardizing ADOS scores for a measure of severity in autism spectrum disorders. J Autism Dev Disord. 39:693–705.

Gould SJ. 1981. Measuring heads. The Mismeasure of Man. New York: WW Norton, 73–112.

Gregory MD, Kippenhan JS, Dickinson D, Carrasco J, Mattay VS, Weinberger DR, Berman KF. 2016. Regional variations in brain gyrification are associated with general cognitive ability in humans. Curr Biol. 26:1301–1305.

Grydeland H, Walhovd KB, Tamnes CK, Westlye LT, Fjell AM. 2013. Intracortical myelin links with performance variability across the human lifespan: results from T1- and T2-weighted MRI myelin mapping and diffusion tensor imaging. J Neurosci. 33:18618–18630.

Hagler DJ, Saygin AP, Sereno MI. 2006. Smoothing and cluster thresholding for cortical surface-based group analysis of fMRI data. Neuroimage. 33:1093–1103.

Han X, Jovicich J, Salat D, van der Kouwe A, Quinn B, Czanner S, Busa E, Pacheco J, Albert M, Killiany R. 2006. Reliability of MRI-derived measurements of human cerebral cortical thickness: the effects of field strength, scanner upgrade and manufacturer. Neuroimage. 32:180–194.

Hardan AY, Jou RJ, Keshavan MS, Varma R, Minshew NJ. 2004. Increased frontal cortical folding in autism: a preliminary MRI study. Psychiatry Res. 131:263–268.

Haxby JV, Hoffman EA, Gobbini MI. 2000. The distributed human neural system for face perception. Trends Cogn Sci. 4:223–233.

Haxby JV, Hoffman EA, Gobbini MI. 2002. Human neural systems for face recognition and social communication. Biol Psychiatry. 51:59–67.

His W. 1874. Unsere Körperform und das physiologische Problem ihrer Enstehung: Briefe an einen Befreundeten Naturforscher: FCW Vogel.

Hogstrom LJ, Westlye LT, Walhovd KB, Fjell AM. 2013. The structure of the cerebral cortex across adult life: age-related patterns of surface area, thickness, and gyrification. Cereb Cortex. 23:2521–2530.

Huttenlocher PR. 1979. Synaptic density in human frontal cortex-developmental changes and effects of aging. Brain Res. 163:195–205.

Huttenlocher PR. 1999. Synaptogenesis in human cerebral cortex and the concept of critical periods. In: Fox NA, Leavitt LA, Warhol JG, editors. The role of early experience in infant development. St. Louis: Johnson & Johnson Pediatric Institute. p. 15–28.

Huttenlocher PR, De Courten C, Garey LJ, Van der Loos H. 1982. Synaptic development in human cerebral cortex. Int J Neurol. 16:144.

Im K, Lee J-M, Lyttelton O, Kim SH, Evans AC, Kim SI. 2008. Brain size and cortical structure in the adult human brain. Cereb Cortex. 18:2181–2191.

Jones GH, Lewis JE. 1991. Head circumference in elderly long-stay patients with schizophrenia. Br J Psychiatry. 159: 435–438.

Jou RJ, Minshew NJ, Keshavan MS, Hardan AY. 2010. Cortical gyrification in autistic and Asperger disorders: a preliminary magnetic resonance imaging study. J Child Neurol. 25: 1462–1467.

Jovicich J, Czanner S, Greve D, Haley E, van der Kouwe A, Gollub R, Kennedy D, Schmitt F, Brown G, MacFall J. 2006. Reliability in multi-site structural MRI studies: effects of gradient non-linearity correction on phantom and human data. Neuroimage. 30:436–443.

Kanwisher N, McDermott J, Chun MM. 1997. The fusiform face area: a module in human extrastriate cortex specialized for face perception. J Neurosci. 17:4302–4311.

Kanwisher N, Yovel G. 2006. The fusiform face area: a cortical region specialized for the perception of faces. Philos Trans R Soc Lond B Biol Sci. 361:2109–2128.

Kates WR, Ikuta I, Burnette CP. 2009. Gyrification patterns in monozygotic twin pairs varying in discordance for autism. Autism Res. 2:267–278.

Klein D, Rotarska-Jagiela A, Genc E, Sritharan S, Mohr H, Roux F, Han CE, Kaiser M, Singer W, Uhlhaas PJ. 2014. Adolescent brain maturation and cortical folding: evidence for reductions in gyrification. PLoS One. 9:e84914.

Kleinhans NM, Richards T, Greenson J, Dawson G, Aylward E. 2016. Altered dynamics of the fMRI response to faces in individuals with autism. J Autism Dev Disord. 46:232–241.

Kleinhans NM, Richards T, Sterling L, Stegbauer KC, Mahurin R, Johnson LC, Greenson J, Dawson G, Aylward E. 2008. Abnormal functional connectivity in autism spectrum disorders during face processing. Brain. 131:1000–1012.

Kochunov P, Robin DA, Royall DR, Coyle T, Lancaster J, Kochunov V, Schlosser AE, Fox PT. 2009. Can structural MRI indices of cerebral integrity track cognitive trends in executive control function during normal maturation and adulthood? Hum Brain Mapp. 30:2581–2594.

Kochunov P, Thompson PM, Coyle TR, Lancaster JL, Kochunov V, Royall D, Mangin JF, Riviere D, Fox PT. 2008. Relationship among neuroimaging indices of cerebral health during normal aging. Hum Brain Mapp. 29:36–45.

Koolschijn PCM, Geurts HM. 2016. Gray matter characteristics in mid and old aged adults with ASD. J Autism Dev Disord. 46:2666–2678.

Koshino H, Kana RK, Keller TA, Cherkassky VL, Minshew NJ, Just MA. 2008. fMRI investigation of working memory for faces in autism: visual coding and underconnectivity with frontal areas. Cereb Cortex. 18:289–300.

Lai M-C, Lombardo MV, Suckling J, Ruigrok AN, Chakrabarti B, Ecker C, Deoni SC, Craig MC, Murphy DG, Bullmore ET. 2013. Biological sex affects the neurobiology of autism. Brain. 136: 2799–2815.

Lainhart JE, Bigler ED, Bocian M, Coon H, Dinh E, Dawson G, Deutsch CK, Dunn M, Estes A, Tager-Flusberg H. 2006. Head circumference and height in autism: a study by the Collaborative Program of Excellence in Autism. Am J Med Genet A. 140:2257–2274.

Lainhart JE, Piven J, Wzorek M, Landa R, Santangelo SL, Coon H, Folstein SE. 1997. Macrocephaly in children and adults with autism. J Am Acad Child Adolesc Psychiatry. 36:282–290.

Lam KS, Aman MG. 2007. The Repetitive Behavior Scale-Revised: independent validation in individuals with autism spectrum disorders. J Autism Dev Disord. 37:855–866.

Levitt JG, Blanton RE, Smalley S, Thompson P, Guthrie D, McCracken JT, Sadoun T, Heinichen L, Toga AW. 2003. Cortical sulcal maps in autism. Cereb Cortex. 13:728–735.

Li G, Wang L, Shi F, Lyall AE, Lin W, Gilmore JH, Shen D. 2014. Mapping longitudinal development of local cortical gyrification in infants from birth to 2 years of age. J Neurosci. 34: 4228–4238.

Libero LE, DeRamus TP, Deshpande HD, Kana RK. 2014. Surface-based morphometry of the cortical architecture of autism spectrum disorders: volume, thickness, area, and gyrification. Neuropsychologia. 62:1–10.

Libero LE, Nordahl CW, Li DD, Ferrer E, Rogers SJ, Amaral DG. 2016. Persistence of megalencephaly in a subgroup of young boys with autism spectrum disorder. Autism Res. 9: 1169–1182.

Lord C, Risi S, Lambrecht L, Cook EH Jr, Leventhal BL, DiLavore PC, Pickles A, Rutter M. 2000. The Autism Diagnostic Observation Schedule-Generic: a standard measure of social and communication deficits associated with the spectrum of autism. J Autism Dev Disord. 30:205–223.

Lord C, Rutter M, Le Couteur A. 1994. Autism Diagnostic Interview-Revised: a revised version of a diagnostic interview for caregivers of individuals with possible pervasive developmental disorders. J Autism Dev Disord. 24: 659–685.

Lynn AC, Padmanabhan A, Simmonds D, Foran W, Hallquist MN, Luna B, O'Hearn K. 2016. Functional connectivity differences in autism during face and car recognition: underconnectivity and atypical age-related changes. Dev Sci. 21:1–18.

Magnotta VA, Andreasen NC, Schultz SK, Harris G, Cizadlo T, Heckel D, Nopoulos P, Flaum M. 1999. Quantitative in vivo measurement of gyrification in the human brain: changes associated with aging. Cereb Cortex. 9:151–160.

McCarthy G, Puce A, Gore JC, Allison T. 1997. Face-specific processing in the human fusiform gyrus. J Cogn Neurosci. 9: 605–610.

Miles JH, Hadden L, Takahashi T, Hillman R. 2000. Head circumference is an independent clinical finding associated with autism. Am J Med Genet. 95:339–350.

Mota B, Herculano-Houzel S. 2012. How the cortex gets its folds: an inside-out, connectivity-driven model for the scaling of mammalian cortical folding. Front Neuroanat. 6:3.

Mullen EM. 1995. Mullen scales of early learning. Circle Pines, MN: AGS.

Mutlu AK, Schneider M, Debbané M, Badoud D, Eliez S, Schaer M. 2013. Sex differences in thickness, and folding developments throughout the cortex. Neuroimage. 82:200–207.

Nordahl CW, Braunschweig D, Iosif A-M, Lee A, Rogers S, Ashwood P, Amaral DG, Van de Water J. 2013. Maternal autoantibodies are associated with abnormal brain enlargement in a subgroup of children with autism spectrum disorder. Brain Behav Immun. 30:61–65.

Nordahl CW, Dierker D, Mostafavi I, Schumann CM, Rivera SM, Amaral DG, Van Essen DC. 2007. Cortical folding abnormalities in autism revealed by surface-based morphometry. J Neurosci. 27:11725–11735.

Nordahl CW, Iosif A-M, Young GS, Perry LM, Dougherty R, Lee A, Li D, Buonocore MH, Simon T, Rogers S, et al. 2015. Sex differences in the corpus callosum in preschool-aged children with autism spectrum disorder. Mol Autism. 6:26.

Nordahl CW, Lange N, Li DD, Barnett LA, Lee A, Buonocore MH, Simon TJ, Rogers S, Ozonoff S, Amaral DG. 2011. Brain enlargement is associated with regression in preschool-age boys with autism spectrum disorders. Proc Natl Acad Sci USA. 108:20195–20200.

Nordahl CW, Scholz R, Yang X, Buonocore MH, Simon T, Rogers S, Amaral DG. 2012. Increased rate of amygdala growth in children aged 2 to 4 years with autism spectrum disorders: a longitudinal study. Arch Gen Psychiatry. 69:53–61.

Nordahl CW, Simon TJ, Zierhut C, Solomon M, Rogers SJ, Amaral DG. 2008. Brief report: methods for acquiring structural MRI data in very young children with autism without the use of sedation. J Autism Dev Disord. 38:1581–1590.

Oblak AL, Rosene DL, Kemper TL, Bauman ML, Blatt GJ. 2011. Altered posterior cingulate cortical cyctoarchitecture, but normal density of neurons and interneurons in the posterior cingulate cortex and fusiform gyrus in autism. Autism Res. 4:200–211.

Ohta H, Nordahl CW, Iosif AM, Lee A, Rogers S, Amaral DG. 2015. Increased surface area, but not cortical thickness, in a subset of young boys with autism spectrum disorder. Autism Res. 9:232–248.

Pakkenberg B, Gundersen HJG. 1997. Neocortical neuron number in humans: effect of sex and age. J Comp Neurol. 384: 312–320.

Paus T, Collins DL, Evans AC, Leonard G, Pike B, Zijdenbos A. 2001. Maturation of white matter in the human brain: a review of magnetic resonance studies. Brain Res Bull. 54: 255–266.

Petanjek Z, Judaš M, Šimić G, Rašin MR, Uylings HB, Rakic P, Kostović I. 2011. Extraordinary neoteny of synaptic spines in the human prefrontal cortex. Proc Natl Acad Sci. 108: 13281–13286.

Pienaar R, Fischl B, Caviness V, Makris N, Grant PE. 2008. A methodology for analyzing curvature in the developing brain from preterm to adult. Int J Imaging Syst Technol. 18: 42–68.

Pierce K, Müller R-A, Ambrose J, Allen G, Courchesne E. 2001. Face processing occurs outside the fusiformface area in autism: evidence from functional MRI. Brain. 124:2059–2073.

Piggot J, Kwon H, Mobbs D, Blasey C, Lotspeich L, Menon V, Bookheimer S, Reiss AL. 2004. Emotional attribution in high-functioning individuals with autistic spectrum disorder: a functional imaging study. J Am Acad Child Adolesc Psychiatry. 43:473–480.

Piven J, Arndt S, Bailey J, Havercamp S, Andreasen NC, Palmer P. 1995. An MRI study of brain size in autism. Am J Psychiatry. 152:1145–1149.

Rajkowska G, Goldman-Rakic PS. 1995. Cytoarchitectonic definition of prefrontal areas in the normal human cortex: I. Remapping of areas 9 and 46 using quantitative criteria. Cereb Cortex. 5:307–322.

Redcay E, Courchesne E. 2005. When is the brain enlarged in autism? A meta-analysis of all brain size reports. Biol Psychiatry. 58:1–9.

Rettmann ME, Kraut MA, Prince JL, Resnick SM. 2005. Cross-sectional and longitudinal analyses of anatomical sulcal changes associated with aging. Cereb Cortex. 16:1584–1594.

Retzius G. 1891. Ueber den Bau der Oberflächenschicht der Grosshirnrinde beim Menschen und bei den Säugethieren: Aftonbladets Aktiebolags tryckeri.

Reuter M, Schmansky NJ, Rosas HD, Fischl B. 2012. Within-subject template estimation for unbiased longitudinal image analysis. Neuroimage. 61:1402–1418.

Richman DP, Stewart RM, Hutchinson JW, Caviness VS. 1975. Mechanical model of brain convolutional development. Science. 189:18–21.

Ronan L, Voets N, Rua C, Alexander-Bloch A, Hough M, Mackay C, Crow TJ, James A, Giedd JN, Fletcher PC. 2014. Differential tangential expansion as a mechanism for cortical gyrification. Cereb Cortex. 24:2219–2228.

Rutter M, Bailey A, Lord C. 2003. The social communication questionnaire (SCQ): manual. Los Angeles. CA: Western Psychological Services.

Sahyoun CP, Belliveau JW, Soulières I, Schwartz S, Mody M. 2010. Neuroimaging of the functional and structural networks underlying visuospatial vs. linguistic reasoning in high-functioning autism. Neuropsychologia. 48:86–95.

Schaer M, Cuadra MB, Schmansky N, Fischl B, Thiran J-P, Eliez S. 2012. How to measure cortical folding from MR images: a step-by-step tutorial to compute local gyrification index. J Vis Exp. 59:e3417.

Schaer M, Cuadra MB, Tamarit L, Lazeyras F, Eliez S, Thiran J. 2008. A surface-based approach to quantify local cortical gyrification. IEEE Trans Med Imaging. 27:161–170.

Schaer M, Kochalka J, Padmanabhan A, Supekar K, Menon V. 2015. Sex differences in cortical volume and gyrification in autism. Mol Autism. 6:1.

Schaer M, Ottet M-C, Scariati E, Dukes D, Franchini M, Eliez S, Glaser B. 2013. Decreased frontal gyrification correlates with altered connectivity in children with autism. Front Hum Neurosci. 7:750.

Schultz RT, Gauthier I, Klin A, Fulbright RK, Anderson AW, Volkmar F, Skudlarski P, Lacadie C, Cohen DJ, Gore JC. 2000. Abnormal ventral temporal cortical activity during face discrimination among individuals with autism and Asperger syndrome. Arch Gen Psychiatry. 57:331–340.

Shokouhi M, Williams JH, Waiter GD, Condon B. 2012. Changes in the sulcal size associated with autism spectrum disorder revealed by sulcal morphometry. Autism Res. 5:245–252.

Sidman RL, Rakic P. 1973. Neuronal migration, with special reference to developing human brain: a review. Brain Res. 62: 1–35.

Sparrow SS, Cicchetti DV, Balla DA. 1989. The vineland adaptive behavior scales. Circle Pines, MN: Americal Guidance Association. 2:199–231.

Ségonne F, Dale A, Busa E, Glessner M, Salat D, Hahn H, Fischl B. 2004. A hybrid approach to the skull stripping problem in MRI. Neuroimage. 22:1060–1075.

Tau GZ, Peterson BS. 2010. Normal development of brain circuits. Neuropsychopharmacology. 35:147–168.

Todd PH. 2013. Intrinsic geometry of biological surface growth. Lecture notes in biomathematics. vol 67. Berlin: Springer Science & Business Media.

Toro R, Burnod Y. 2005. A morphogenetic model for the development of cortical convolutions. Cereb Cortex. 15:1900–1913.

Van Essen DC. 1997. A tension-based theory of morphogenesis and compact wiring in the central nervous system. Nature. 385:313–318.

van Kooten IA, Palmen SJ, von Cappeln P, Steinbusch HW, Korr H, Heinsen H, Hof PR, van Engeland H, Schmitz C. 2008. Neurons in the fusiform gyrus are fewer and smaller in autism. Brain. 131:987–999.

Wallace GL, Robustelli B, Dankner N, Kenworthy L, Giedd JN, Martin A. 2013. Increased gyrification, but comparable surface area in adolescents with autism spectrum disorders. Brain. 136:1956–1967.

Wang AT, Dapretto M, Hariri AR, Sigman M, Bookheimer SY. 2004. Neural correlates of facial affect processing in children and adolescents with autism spectrum disorder. J Am Acad Child Adolesc Psychiatry. 43:481–490.

Webb SJ, Monk CS, Nelson CA. 2001. Mechanisms of postnatal neurobiological development: implications for human development. Dev Neuropsychol. 19:147–171.

Weigelt S, Koldewyn K, Kanwisher N. 2012. Face identity recognition in autism spectrum disorders: a review of behavioral studies. Neurosci Biobehav Rev. 36:1060–1084.

Weinberg WA, Dietz SG, Penick EC, McAlister WH. 1974. Intelligence, reading achievement, physical size, and social class: a study of St. Louis Caucasian boys aged 8-0 to 9–6 years, attending regular schools. the Journal of Pediatrics. 85:482–489.

White T, Su S, Schmidt M, Kao C-Y, Sapiro G. 2010. The development of gyrification in childhood and adolescence. Brain Cogn. 72:36–45.

Whyte EM, Behrmann M, Minshew NJ, Garcia NV, Scherf KS. 2016. Animal, but not human, faces engage the distributed face network in adolescents with autism. Dev Sci. 19: 306–317.

Yang DY-J, Beam D, Pelphrey KA, Abdullahi S, Jou RJ. 2016. Cortical morphological markers in children with autism: a structural magnetic resonance imaging study of thickness, area, volume, and gyrification. Mol Autism. 7:1.